Journal of Aeronautics & Aerospace Engineering
ISSN: 2168-9792

Kumar et al., J Aeronaut Aerospace Eng 2016, 5:2
DOI: 10.4172/2168-9792.1000171

Research Article Open Access

Aerodynamic Analysis of Multi Element Airfoil

Udaya Kumar D*, Kannan S, Vimal Chand D, Sriram R and Ganapathi C

Aeronautical Jeppiaar Engineering College, Chennai, India

Abstract

The flow over multi-element airfoils has been numerically investigated in ANSYS fluent and has been compare the aerodynamic parameters with the standard NACA airfoils 4412 and 0012. The 2D viscous, transient, pressure model equations together with the k-ω turbulence model were applied to this numerical simulation utilizing the multi-block unstructured grids of sphere of influence type. Numerical results showed that the aerodynamic parameters of multi element airfoils with tail effect are much optimum than the standard NACA airfoils. Also the analysis is made on different flap and slat angles of different conditions and the optimization of multi element airfoils has been performed.

Keywords: High lift devices; Multi-element airfoils; Lift co-efficient; Structured grid

Introduction

The High-lift capability of an aircraft, affecting take-off and landing performance and low-speed maneuverability, plays an important role in the design of military and commercial aircraft. Improved high-lift performance can lead to increased range and payload as well as decreased landing speed and field length requirements. The take-off configuration designed for a high lift-to-drag ratio (L/D) at moderate lift coefficient is different from the landing configuration designed for high maximum lift coefficient. Typical high-lift system for transport aircraft often consisting o f a basic wing with a leading-edge slat and trailing-edge flap elements is highly efficient aerodynamically, but at the expense of complex structure and expensive design and maintenance costs. Current design effects have focused on mechanically simpler which maximum lift occurs is about 23°, which is slightly larger than that of experiment.

The figures plot the pressure coefficient on the surface of the elements at 16 angles of attack comparing computational results against experimental results. As can be seen from the figure, computed pressure distribution is in very good agreement with measurements.

It's worth mentioning that the computed results showed traces of small flow separation on the upper surface of the flap at angles of attack below 12° and off-body separation in the wake of the main element at angles of attack above 20° and fully attachment over the flap at all other angles of attack. High-lift systems that incorporate advanced technology to meet design requirements [1-5].

Numerical Methods and Mesh

The 2D unsteady Reynolds-Averaged Navier- Stokes (RANS) equations were applied to this numerical simulation using the finite volume method. The discretized schemes of the convective fluxes, diffusive fluxes and unsteady terms were all of second-order accuracy and the resulting equations were solved with simple scheme. In this study, fully turbulent computations were performed using the k-ω turbulence model. In addition to no-slip wall boundary condition applied at the airfoil surface, pressure far field boundary condition was used.

In the present simulation the airfoil is NACA 4412, the free stream velocity is set at 10 m/s and Reynolds number based on chord length is 7.03×10^5. This NACA airfoil can be analyzed with different angle of attack up to 14 and the aerodynamic performance has been computed such as cl vs. alpha, cd vs. cl and monitors the pressure, velocity and vorticity contours. Similarly, the NACA 0012 airfoils have been analyzed at different angle of attacks. As for computational domain, the upstream and downstream distances from the airfoil were 12.5 reference chords.

Similarly the multi element airfoil 30P30N has been analyzed with tail airfoils at different flap and slat angles for different flight conditions and can be compared with optimum aerodynamic data. The mesh topology used for the standard NACA airfoils is C highly complex structured grid. It has the advantage of highly convergence criteria and high mesh topology. The multi block unstructured grid is used for multi element airfoil with fine mesh using sphere of influence method [6-10].

The baseline configuration of MDA three- element airfoil 30P30N, as shown in Figure 1, is used here as a validation case of numerical methods. Many efforts of multi-element airfoils computation have been made to various MDA three-element configurations, tested over the course of many years (primarily the 1990s) in the NASA Langley LTPT. For the 30P30N configuration with both slat and flap deflected 30°, the slat overlap and gap defined in Fig.1 are -2.50 and 2.95 percent of undeflected airfoil chord, and the flap overlap and gap are 0.25 and 0.89 percent respectively. A closed-up of the computational grid is shown in Figure 2.

A comparison of computed and experimental lift coefficient versus angle of attack is shown in Figure 3. Excellent agreement with experiment is obtained for the lift coefficient at lower angles of attack, and the discrepancy in maximum lift coefficient between computation and experiment is less than 2.7%. The computed angle of attack at which maximum lift occurs is about 23°, which is slightly larger than that of experiment.

Figure 4 plots the pressure coefficient on the surface of the elements at 16 angles of attack comparing computational results

***Corresponding author:** Udaya Kumar D, Assistant Professor, Aeronautical Jeppiaar Engineering College, Chennai, India, Tel: 044 2450 2818; E-mail: udayarvi@gmail.com

Received June 14, 2016; **Accepted** June 29, 2016; **Published** June 30, 2016

Citation: Kumar DU, Kannan S, Vimal Chand D, Sriram R, Ganapathi C (2016) Aerodynamic Analysis of Multi Element Airfoil. J Aeronaut Aerospace Eng 5: 171. doi:10.4172/2168-9792.1000171

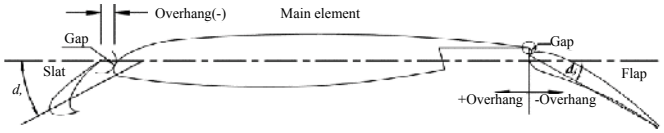

Figure 1: Multi element airfoil.

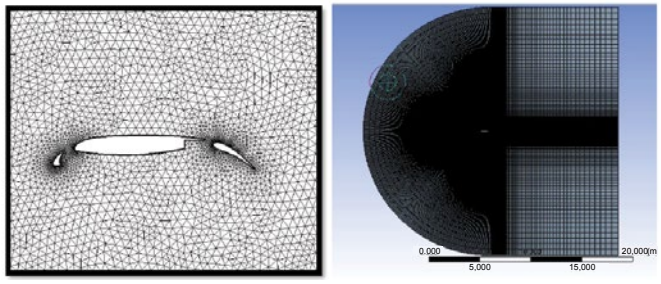

Figure 2: Mesh.

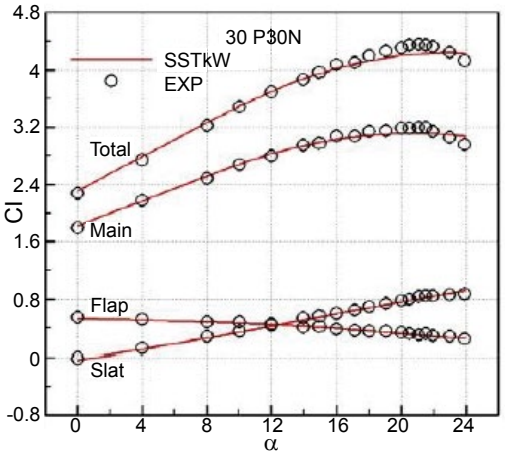

Figure 3: Comparison of lift coefficient for 30P30N between computation and experiment.

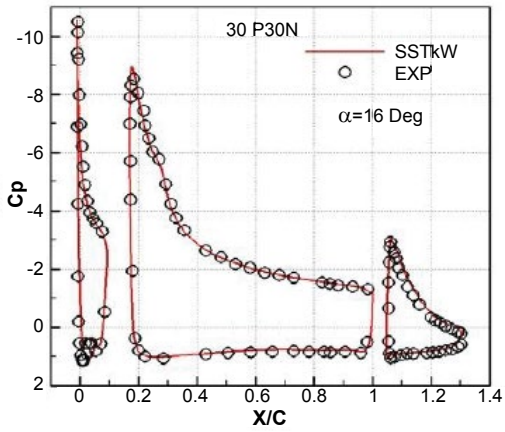

Figure 4: Comparison of computational and experimental pressure distribution for 30P30N.

against experimental results. As can be seen from the figure, computed pressure distribution is in very good agreement with measurements.

It's worth mentioning that the computed results showed traces of small flow separation on the upper surface of the flap at angles of attack below 12°, and off-body separation in the wake of the main element at angles of attack above 20°, and fully attachment over the flap at all other angles of attack.

Results and Discussion

Lift behaviour

First we discuss the standard NACA airfoils of 0012 and 4412 in which the lift coefficient varies with the linearly of different angle of attack up to which stalls at 12 to 14 degree. This is the standard configurations airfoils that have used for low subsonic aircrafts (Figure 5). But these airfoils cannot be used at different flight conditions to optimize the lift coefficient. But the multi element airfoil has been attached to the wing so that it increases the lift coefficient by delaying the flow separation in the surface and makes the flow smooth so that it can be optimize the lift coefficient.

The angles has been varied and analyzed at flow inlet velocity conditions of 10m/s in which at the stalling has been increased in the NACA 4412 airfoils and the cl vs. alpha graph has been shown in Figure 6. From the graph we know that, the stalling angle of the NACA 4412 airfoils has in the range of 14 to 16 degree in which the separation of boundary layer occurs. Thus compared to standard airfoil with multi element, the delay of separation is high in multi element airfoil.

The pressure coefficient over the airfoil has been modified when the multi element airfoil has been used so that it has improved his aerodynamic efficiency of the wing rather than the conventional airfoil.

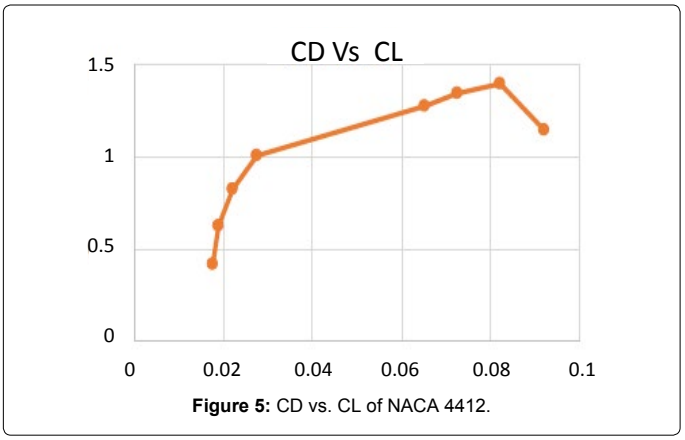

Figure 5: CD vs. CL of NACA 4412.

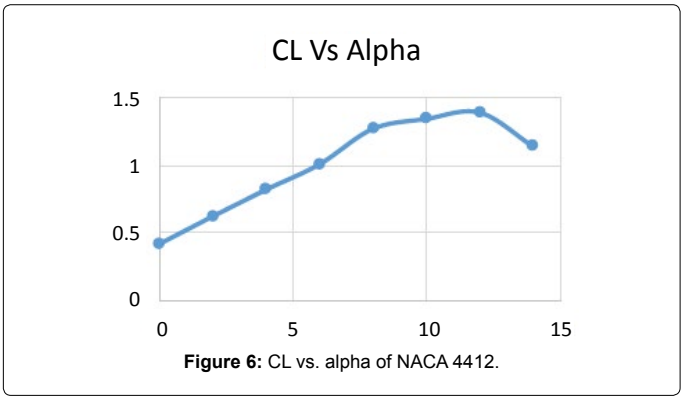

Figure 6: CL vs. alpha of NACA 4412.

Drag behaviour

The multi element airfoil has been numerically investigated so that the drag coefficient is higher at the high subsonic cruise conditions in which the flow separation becomes more turbulence than the conventional airfoil at high speeds. This shows that the multi element airfoil is optimum at low subsonic cruise conditions which is shown in the graph (Figure 5).

Pressure coefficient

The pressure coefficients of NACA 4412 and 0012 with different angle of attacks shown in Figures 5 and 6. The pressure coefficient is defined by the equation:

$$C_p = \frac{p - p_\infty}{\frac{1}{2} p_\infty V_\infty^2}$$

In many aerodynamic problems where one is primarily interested in lift, the work done by external forces such as gravity and viscous forces is neglected. For incompressible flow, the Cp at stagnation point is 1. In this investigation, Cp is much larger than 1 on the pressure surface. The explanation of this result is given below.

Thus the pressure coefficient of multi element airfoil at different configurations as has shown in Figure 7 and compared with the standard NACA airfoils of 4412 pressure coefficient which is shown in Figures 8 and 9.

Flow field and discussion

In this section, the contours values (Pressure, Velocity, vorticity) of different airfoils are measured and the figures present below Figures 10-12 represent the respective values. Figure 8 shows that NACA 4412 has high lift co-efficient, and more stalling angle, less flow separation with less downwash effect when compared to the NACA 0012.

Then the multi element airfoil is analyzed at different conditions and the results shows that the separation is delayed by changing the deflection of slats and flaps. Then the NACA standard airfoil is attached to the multi element airfoil and the aerodynamic lift coefficient has been increases and the flow separation has been reduced by delaying the transition point from laminar to turbulent flow.

The location of the separation point on the flap upper surface is nearly identical to that of baseline configuration at 8° angle of attack. However, at 0° angle of attack the computed results not reported here showed that the separation point moved downstream slightly toward the trailing edge of flap. The change in drag coefficient can be negligible

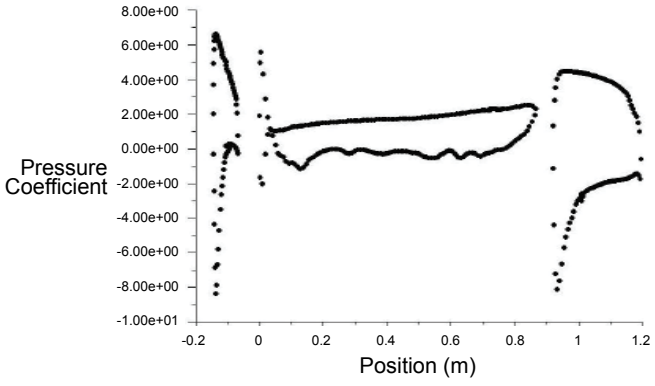

Figure 7: Pressure coefficient of multi-element airfoil.

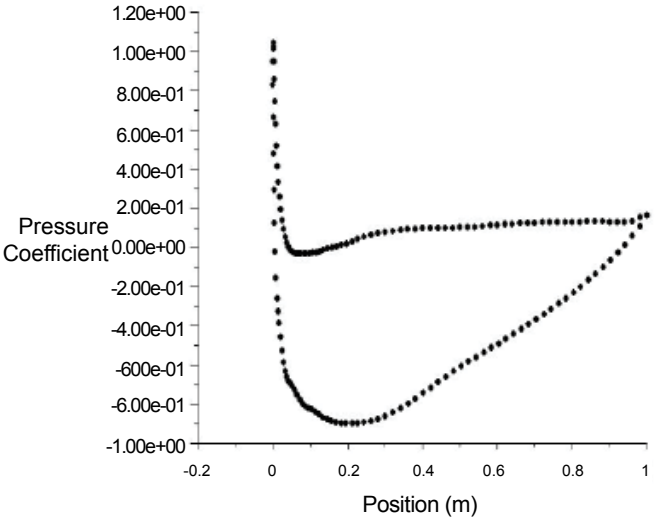

Figure 8: Pressure coefficient of NACA 4412.

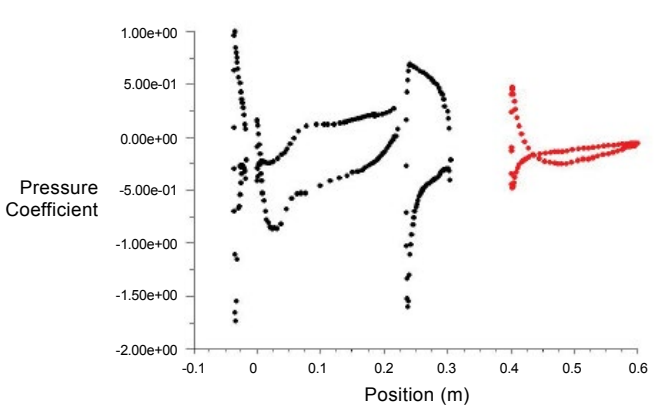

Figure 9: Pressure coefficient of multi-element airfoil with standard airfoil.

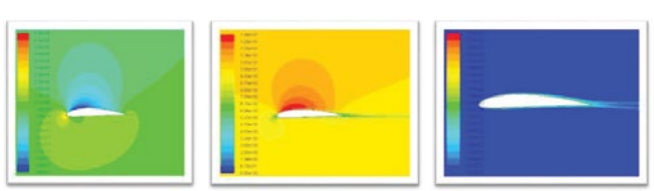

Figure 10: NACA 4412 airfoil contours-pressure, velocity and vorticity.

compared to the baseline configuration. The addition of a flap tab to the baseline configuration shifts the pitching moment coefficient curve in the negative direction.

Conclusion

CFD simulations are employed to study the flow field and the aerodynamic properties of a NACA 4412 and 0012 airfoil. First, the accuracy of the numerical method is validated by computing the flow past multi element with standard tail effect and comparing the results with experimental data. Then, the flow fields around the airfoil and the multi element airfoil are discussed. From the analysis of the flow properties and aerodynamic forces, it is found that multi element with

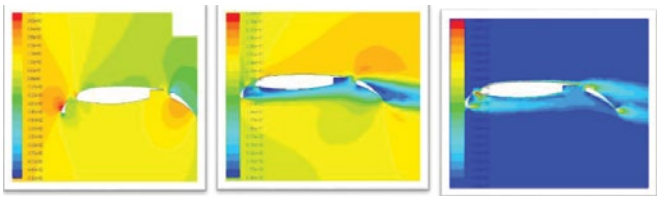

Figure 11: Multi element airfoil contours-pressure, velocity and vorticity.

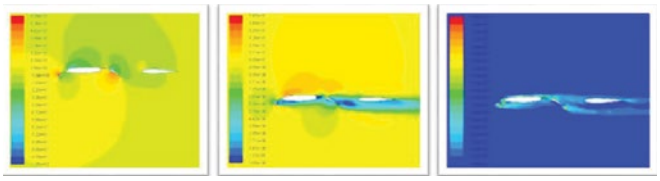

Figure 12: Multi element airfoil with NACA 0012 airfoil contours-pressure, velocity and vorticity.

tail airfoil has better aerodynamic efficiency at different flap and slat configurations than the conventional standard airfoils. Hence it is used has high lift devices in the wing section that has increase the overall lift coefficient of the wing.

References

1. Valarazo WO, Dominik CJ, McGhee RJ, Goodman WL (1992) High Reynolds number configuration development of a high-lift airfoil. AGARD Conference Proceedings of High-lift Systems Aerodynamics.
2. Anderson WK, Bonhaus DL, McGhee R, Walker B (1995) Navier-Stokes computations and experimental comparisons for multi-element airfoil configurations. J Aircraft 32: 1246-1253.
3. Yang Z, Igarashi H, Martin M, Hu H (2008) An experimental investigation on aerodynamic hysteresis of a low-Reynolds number airfoil AIAA.
4. Smith AMO (1975) High-lift aerodynamics. J Aircraft 12: 501-530.
5. Ahmed MR, Takasaki T, Kohama Y (2007) Aerodynamics of a NACA 4412 airfoil in ground effect AIAA 45: 37-47.
6. Storms BL, Ross JC (1994) An experimental study of lift-enhancing tabs on a two-element airfoil. AIAA 32: 1072-1078.
7. Chin VD, Peters DW, Spaid FW, McGhee RJ (1993) Flow-field measurements about a multi-element airfoil at high Reynolds numbers. AIAA Paper 93- 3137.
8. Singh MK, Dhanalakshmi K, Chakrabartty SK (2007) Navier–stokes analysis of airfoils with gurney flap. J Aircraft. 44:1487- 1493.
9. Klausmeyer SM, Papadakis M, Lin JC (1996) A flow physics study of vortex generators on a multi- element airfoil. AIAA Paper 96-0548.
10. Brunet V, Garnier E, Pruvost M (2006) Experimental and numerical investigations of vortex generators effects. 3rd AIAA Conference on Fluid Dynamics, California.